Electronic Supplementary Material (ESI) for Physical Chemistry Chemical Physics.

Supplementary Information.

Active learning-based framework for optimal reaction mechanism selection from microkinetic modeling: A case study of electrocatalytic oxygen reduction reaction on carbon nanotubes

Aleksandr A. Kurilovich[a], Caleb T. Alexander[b], Egor M. Pazhetnov[a], and Keith J. Stevenson[*a]

a Skolkovo Institute of Science and Technology, Skolkovo Innovation Center, Building 3, Moscow, 143026, Russian Federation.

b 12318 Mossycup Dr. Houston, Texas 77024, USA.

Mean-field microkinetic modeling details.

Flat electrode surface with uniformly distributed carbon active sites, which are equally accessible for O_2 and HO_2^- species was considered in simulations. The concentration profile on the vicinity of the electrode surface was assumed to be linear for O_2 and HO_2^- species. The diffusion in the bulk of the electrode was neglected because of the low catalyst loadings.

Then the effective diffusion layer thickness δ_{O_2,HO_2^-} {cm} for O_2 and HO_2^- is evaluated from the approximate analytical solution for RDE reported by Levich[1].

$$\delta_{O_2,HO_2^-} = 1.61 D_{O_2,HO_2^-}^{1/3} \nu^{1/6} \omega^{-1/2}$$

Here, D_{O_2,HO_2^-} {$cm^2\ s^{-1}$} are diffusivities of O_2 and HO_2^- respectively, ν {$cm^2\ s^{-1}$} – kinematic viscosity, ω {$rad\ s^{-1}$} – RDE rotation rate. The values for D_{O_2,HO_2^-} and ν were taken from literature data[2].

All rate constant values are reported for the 0.1 M KOH solution. The rate constants for effective $2e^-$ charge transfer steps are given at E_0 = 0.7404 V vs. RHE. Prior to each numerical solution, the backward rate constant value for the charge transfer step was numerically calculated to reproduce the standard potential of O_2/HO_2^- redox pair in alkaline media.

Model (a)

Three steps are considered within this model.

1) Oxygen adsorption/desorption step on/from the surface:

$$v_{1a}: * + O_2 \rightarrow O_{2ads} \quad (S1)$$

2) Effective $2e^-$ reduction/oxidation step of/to O_2 to/from HO_2^-. Reaction product remains adsorbed on the surface:

$$v_{2a}: O_{2ads} + H_2O + 2e^- \rightarrow HO_{2_{ads}}^- + OH^- \quad (S2)$$

3) HO_2^- desorption/adsorption step from/on the surface:

$$v_{3a}: HO_{2_{ads}}^- \rightarrow * + HO_2^- \quad (S3)$$

The rates of steps can be formally expressed as follows:

$$v_{1a} = k_{1a} c_{O_2}\left(1 - \theta_{O_2} - \theta_{HO_2^-}\right) - k_{-1a}\theta_{O_2} \quad (S4)$$

$$v_{2a} = k_{2a}\theta_{O_2} exp\left(-\frac{\alpha_{2a}F(E - E_o)}{RT}\right) - k_{-2a}\theta_{HO_2^-} exp\left(\frac{(1-\alpha_{2a})F(E - E_o)}{RT}\right) \quad (S5)$$

$$v_{3a} = k_{3a}\theta_{HO_2^-} - k_{-3a} c_{HO_2^-}\left(1 - \theta_{O_2} - \theta_{HO_2^-}\right) \quad (S6)$$

Here k_{1a}/k_{-1a} {cm^3 mol^{-1} s^{-1}/ s^{-1}} are forward/backward rate constants for reaction step (S1), k_{2a}/k_{-2a} {s^{-1}/ s^{-1}} are forward/backward rate constants for reaction step (S2), α_{2a} {1}- charge transfer coefficient in (S2), k_{3a}/k_{-3a} { s^{-1}/ cm^3 mol^{-1} s^{-1}} are forward/backward rate constants for reaction step (S3), $\theta_{O_2}/\theta_{HO_2^-}$ {1/1} are surface coverages by O_2 and HO_2^- species respectively, E_o – potential at which rate constants for electrochemical step were specified (0.7404 V vs. RHE in this work), R – universal gas constant {J K^{-1} mol^{-1}}, F – Faraday constant {C mol^{-1}}, and T – temperature {K} (298 K in this work).

The model, which was solved numerically:

$$\begin{cases} \dfrac{d\theta_{O_2}}{dt} = 0 = v_{1a} - v_{2a} \\ \dfrac{d\theta_{HO_2^-}}{dt} = 0 = v_{2a} - v_{3a} \\ D_{O_2}\left(\dfrac{dc_{O_2}}{dx}\right)_{x=0} \approx D_{O_2}\dfrac{c_{O_2}^* - c_{O_2}}{\delta_{O_2}} = \Gamma_C v_{1a} \\ D_{HO_2^-}\left(\dfrac{dc_{HO_2^-}}{dx}\right)_{x=0} \approx D_{HO_2^-}\dfrac{c_{HO_2^-}^* - c_{HO_2^-}}{\delta_{HO_2^-}} = -\Gamma_C v_{3a} \end{cases} \quad (S7)$$

Here c_{O_2/HO_2^-} {mol cm^{-3}} are concentrations of O_2 and HO_2^- species in the vicinity of the electrode surface, $c_{O_2/HO_2^-}^*$ {mol cm^{-3}} are concentrations of O_2 and HO_2^- in the bulk of electrolyte, given by oxygen solubility in 0.1 M KOH[3] and experimental conditions for HPRR/HPOR. Γ_C is CNT

active site surface density {mol cm^{-2}}. It was recalculated from the value used in our previous simulations[4] for Vulcan Carbon XC-72 (VC) using the ratios of BET surface areas and mass loadings for VC and CNTs.

If one wants to simulate ORR proceeding within the same reaction mechanism but in non-steady state approximation, then the system of ordinary differential equations should be solved numerically. Linear dependence of RDE potential on time should be introduced. Non-zero time derivatives of surface coverages will be expressed the same way as in (S7). Time-derivatives of surface coverages can be calculated as was shown in[5]

Finally, the geometric current density $I_{geom}(E)$ is evaluated from:

$$I_{geom}(E) = -2F\Gamma_C v_{2a}(E) \quad (S8)$$

Model (b)

This model is obtained by simplification of the Model (a) by merging steps (S2) and (S3). No adsorbed HO_2^- considered (fast HO_2^- adsorption/desorption step).

$$v_{1b}: * + O_2 \rightarrow O_{2ads} \quad (S9)$$

$$v_{2b}: O_{2ads} + H_2O + 2e^- \rightarrow * + HO_2^- + OH^- \quad (S10)$$

Then, the rates will be:

$$v_{1b} = k_{1b}c_{O_2}\left(1 - \theta_{O_2}\right) - k_{-1b}\theta_{O_2} \quad (S11)$$

$$v_{2b} = k_{2b}\theta_{O_2}exp\left(-\frac{\alpha_{2b}F(E - E_o)}{RT}\right) - k_{-2b}c_{HO_2^-}\left(1 - \theta_{O_2}\right)exp\left(\frac{(1 - \alpha_{2b})F(E - E_o)}{RT}\right) (S12)$$

Here k_{1b}/k_{-1b} {$cm^3\ mol^{-1}\ s^{-1}/\ s^{-1}$} are forward/backward rate constants for reaction step (S9), k_{2b}/k_{-2b} {$s^{-1}/\ cm^3\ mol^{-1}\ s^{-1}$} are forward/backward rate constants for reaction step (S10), and α_{2b} {1}- charge transfer coefficient in (S10).

Numerical model:

$$\begin{cases} \dfrac{d\theta_{O_2}}{dt} = 0 = v_{1\mathrm{b}} - v_{2\mathrm{b}} \\ D_{O_2}\left(\dfrac{dc_{O_2}}{dx}\right)_{x=0} \approx D_{O_2}\dfrac{c^*_{O_2} - c_{O_2}}{\delta_{O_2}} = \Gamma_C v_{1b} \\ D_{HO_2^-}\left(\dfrac{dc_{HO_2^-}}{dx}\right)_{x=0} \approx D_{HO_2^-}\dfrac{c^*_{HO_2^-} - c_{HO_2^-}}{\delta_{HO_2^-}} = -\Gamma_C v_{2b} \end{cases} \quad (S13)$$

Geometric current density:

$$I_{geom}(E) = -2F\Gamma_C v_{2\mathrm{b}}(E) \quad (S14)$$

Model (c)

No surface coverages are considered within the simplest single step model:

$$v_{1c}: O_2 + H_2O + 2e^- \rightarrow HO_2^- + OH^- \quad (S15)$$

Reaction rate:

$$v_{1c} = k_{1c}c_{O_2}exp\left(-\frac{\alpha_{1c}F(E-E_o)}{RT}\right) - k_{-1c}c_{HO_2^-}exp\left(\frac{(1-\alpha_{1c})F(E-E_o)}{RT}\right) \quad (S16)$$

Here k_{1c}/k_{-1c} {$cm^3\ mol^{-1}\ s^{-1}/\ cm^3\ mol^{-1}\ s^{-1}$} are forward/backward rate constants for reaction step (S15), and α_{1c} {1}- charge transfer coefficient in (S15).

Numerical model:

$$\begin{cases} D_{O_2}\left(\dfrac{dc_{O_2}}{dx}\right)_{x=0} \approx D_{O_2}\dfrac{c^*_{O_2} - c_{O_2}}{\delta_{O_2}} = \Gamma_C v_{1c} \\ D_{HO_2^-}\left(\dfrac{dc_{HO_2^-}}{dx}\right)_{x=0} \approx D_{HO_2^-}\dfrac{c^*_{HO_2^-} - c_{HO_2^-}}{\delta_{HO_2^-}} = -\Gamma_C v_{1c} \end{cases} \quad (S17)$$

Geometric current density:

$$I_{geom}(E) = -2F\Gamma_C v_{1c}(E) \quad (S18)$$

Supplementary Table 1. Estimated uncertainties of independent model parameters.

Model parameter	Overall parameter sampling interval	ORR fitting. Minimal interval, which contains all parameters giving the accuracy of fitting lower than experimental error.	ORR and HPRR/HPOR fitting. Minimal interval, which contains all parameters giving the accuracy of fitting lower than experimental error.
Model (a)			
k_{1a}, s^{-1} cm^3 mol^{-1}	$3.4x10^{-4}$...$3.4x10^{10}$	$2.8x10^{6}$…$1.3x10^{7}$	$2.8x10^{6}$…$7.2x10^{7}$
k_{-1a}, s^{-1}	$3.4x10^{-4}$...$3.4x10^{10}$	$3.4x10^{0}$…$1.9x10^{8}$	$2.2x10^{0}$...$5.6x10^{7}$
k_{2a}, s^{-1}	$3.4x10^{-4}$...$3.4x10^{10}$	$4.8x10^{-2}$…$2.1x10^{6}$	$2.3x10^{-2}$…$7.2x10^{6}$
k_{3a}, s^{-1}	$3.4x10^{-4}$...$3.4x10^{10}$	$4.4x10^{0}$…$5.3x10^{8}$	$5.5x10^{0}$…$1.7x10^{9}$
k_{-3a}, s^{-1}	$3.4x10^{-4}$...$3.4x10^{10}$	$9.6x10^{0}$…$3.4x10^{10}$	$1.2x10^{1}$…$7.7x10^{9}$
α_{2a}, 1	0.40…0.95	0.40…0.92	0.43…0.90
Model (b)			
k_{1b}, s^{-1} cm^3 mol^{-1}	$3.4x10^{-4}$...$3.4x10^{10}$	$2.8x10^{6}$…$3.9x10^{6}$	$2.8x10^{6}$…$3.5x10^{6}$
k_{-1b}, s^{-1}	$3.4x10^{-4}$...$3.4x10^{10}$	$8.8x10^{0}$…$5.5x10^{2}$	$9.7x10^{0}$…$1.7x10^{2}$
k_{2b}, s^{-1}	$3.4x10^{-4}$...$3.4x10^{10}$	$3.1x10^{-2}$…$5.9x10^{6}$	$3.6x10^{-2}$…$1.5x10^{1}$
α_{2b}, 1	0.40…0.95	0.42…0.91	0.64…0.90

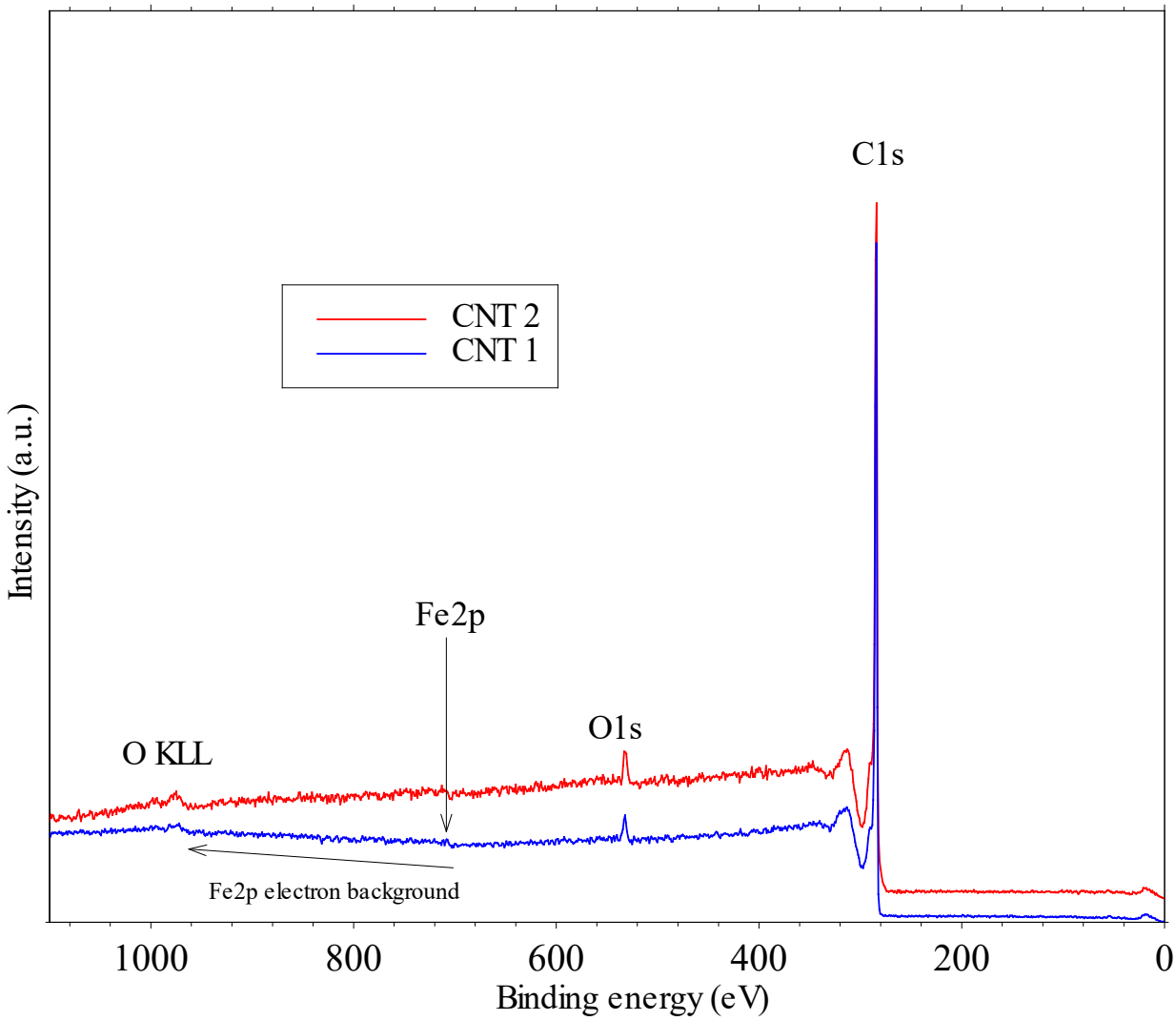

Supplementary Figure 1. XPS survey spectra measured for two multiwalled carbon nanotube materials: CNT 1 sample – studied in [6] and CNT 2 sample – studied in this work. Spectra were shifted in Y-axis for the sake of comparison.

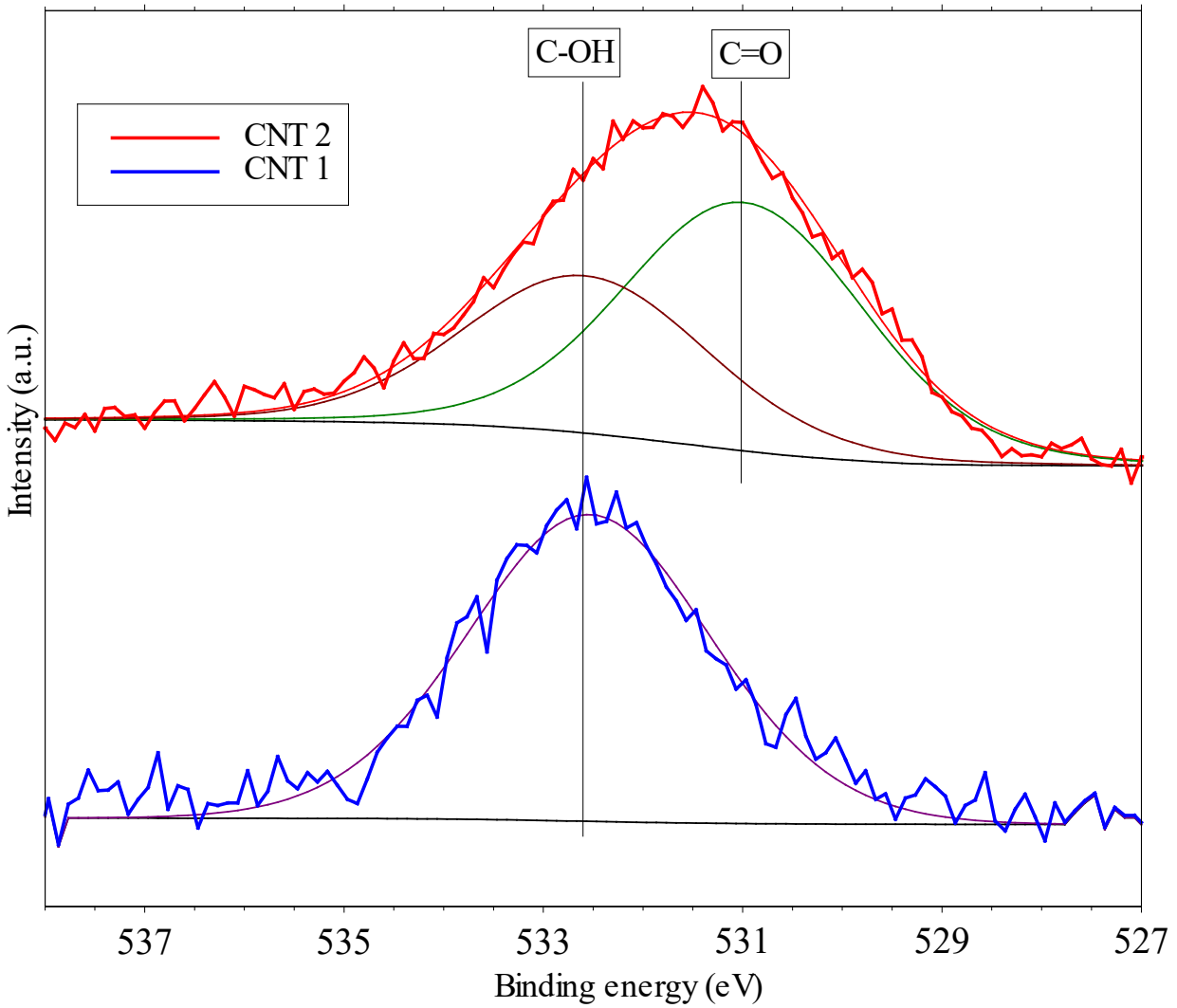

Supplementary Figure 2. O1s high-resolution spectra measured for two multiwalled carbon nanotube materials: CNT 1 sample – studied in [6] and CNT 2 sample – studied in this work. Best peak fitting results. Spectra were shifted in Y-axis for the sake of comparison.

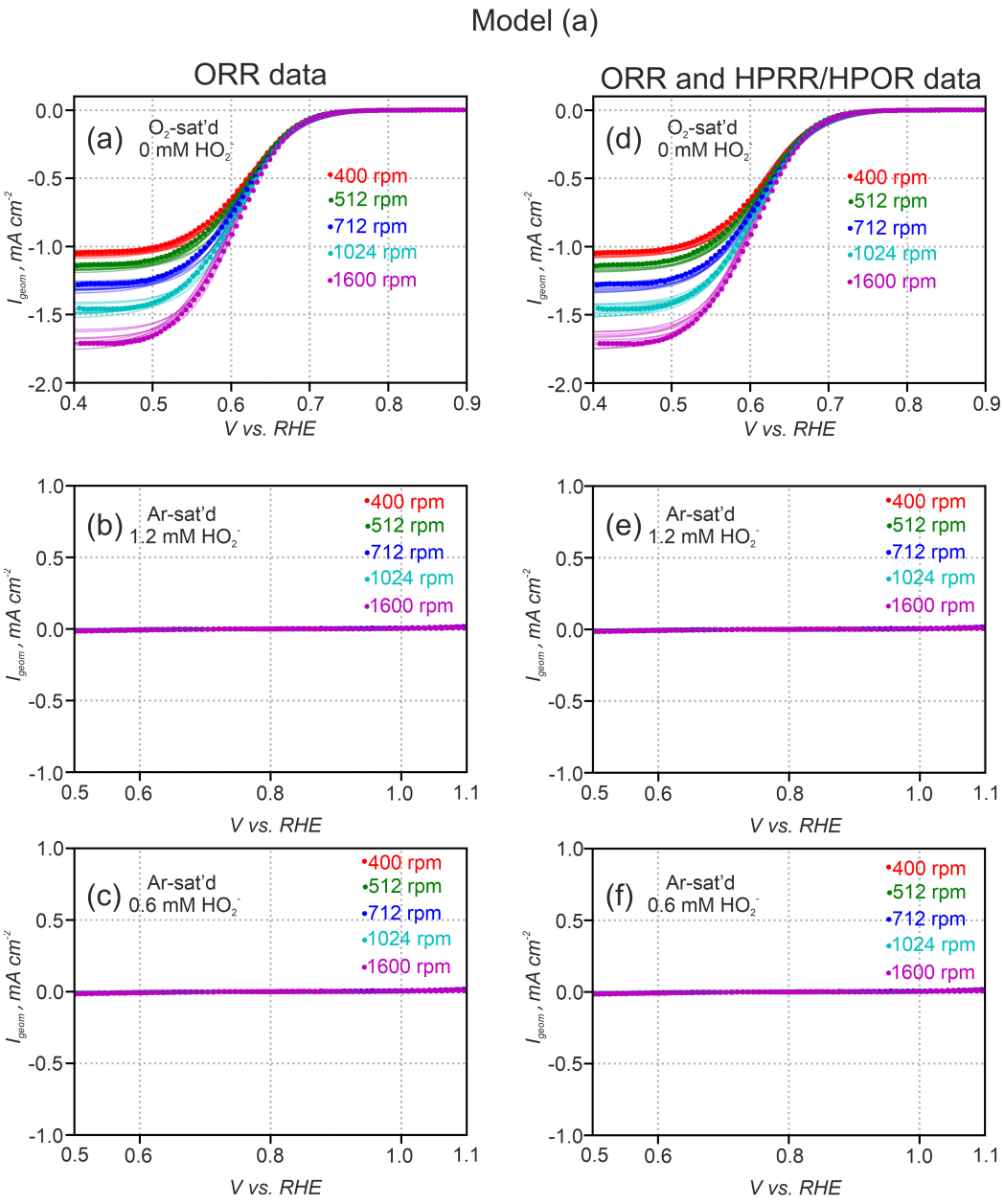

Supplementary Figure 3. Example of modeling results for the model (a) with 3 reaction steps. All figures include the simulated RDE CVs for 10 random sets of model parameters with target functional lower than the experimental error (semi-transparent lines) and averaged experimental data (dots). Model parameters were adjusted by fitting of ORR RDE (a-c) and both ORR and HPRR/HPOR RDE (d-f) data. Simulated RDE CVs for O_2-saturated solution (a, d), Ar-saturated solution with added 1.2 mM (b, e) and 0.6 mM (c, f) of hydroperoxide are shown.

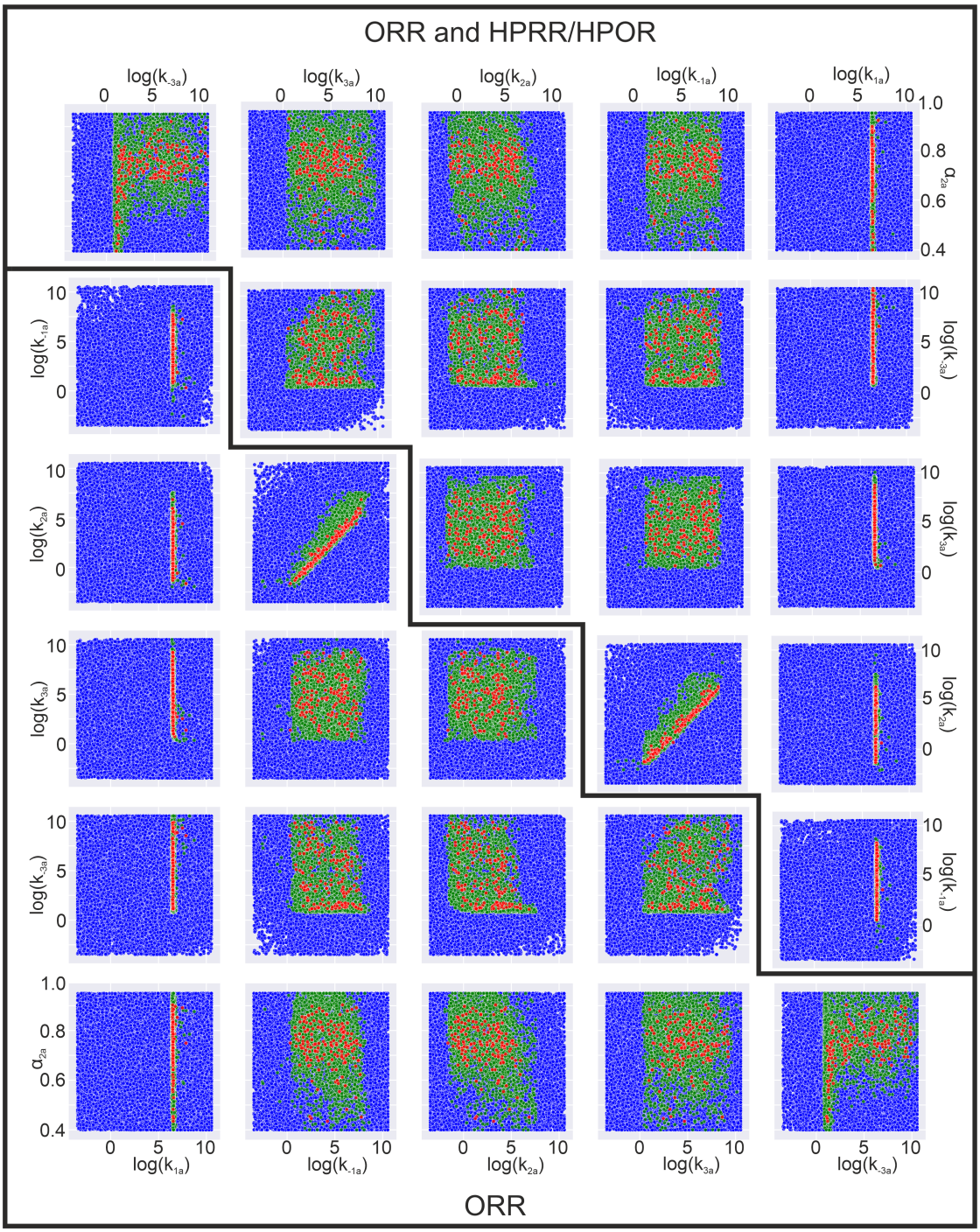

Supplementary Figure 4. Pair distributions of independent model (a) parameters. The figures on the left lower and right upper parts correspond to the fitting of ORR only and all ORR plus HPRR/HPOR RDE CVs respectively. Dots represent sets of the model parameters, for which target function was evaluated to be: lower than experimental error (red); between one and four experimental errors (green); higher than four experimental errors (blue).

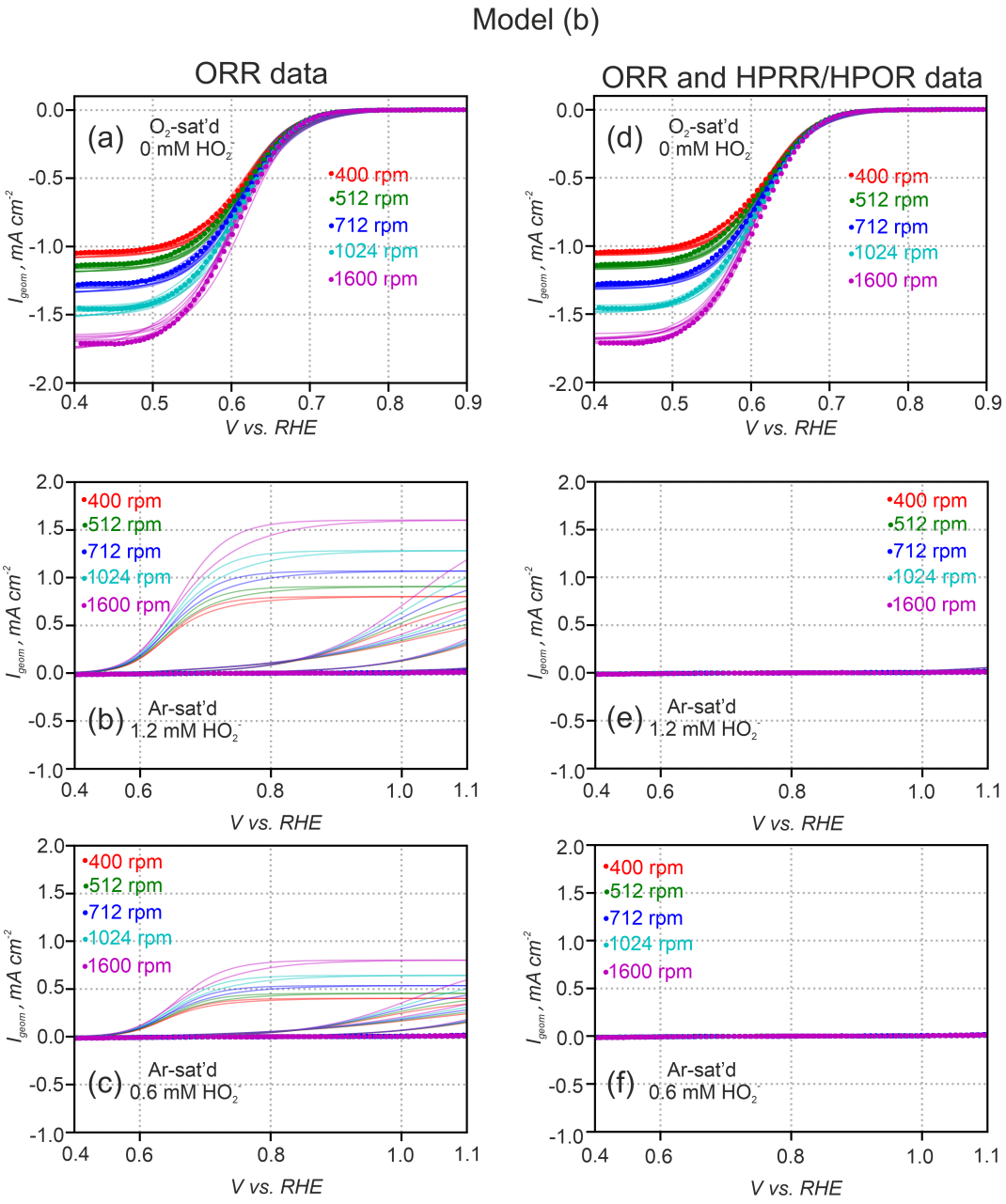

Supplementary Figure 5. Example of modeling results for the model (b) with 2 steps. All figures include the simulated RDE CVs for 10 random sets of model parameters with target functional lower than the experimental error (semi-transparent lines) and averaged experimental data (dots). Model parameters were adjusted by fitting of ORR RDE (a-c) and both ORR and HPRR/HPOR RDE (d-f) data. Simulated RDE CVs for O_2-saturated solution (a, d), Ar-saturated solution with added 1.2 mM (b, e) and 0.6 mM (c, f) of hydroperoxide are shown.

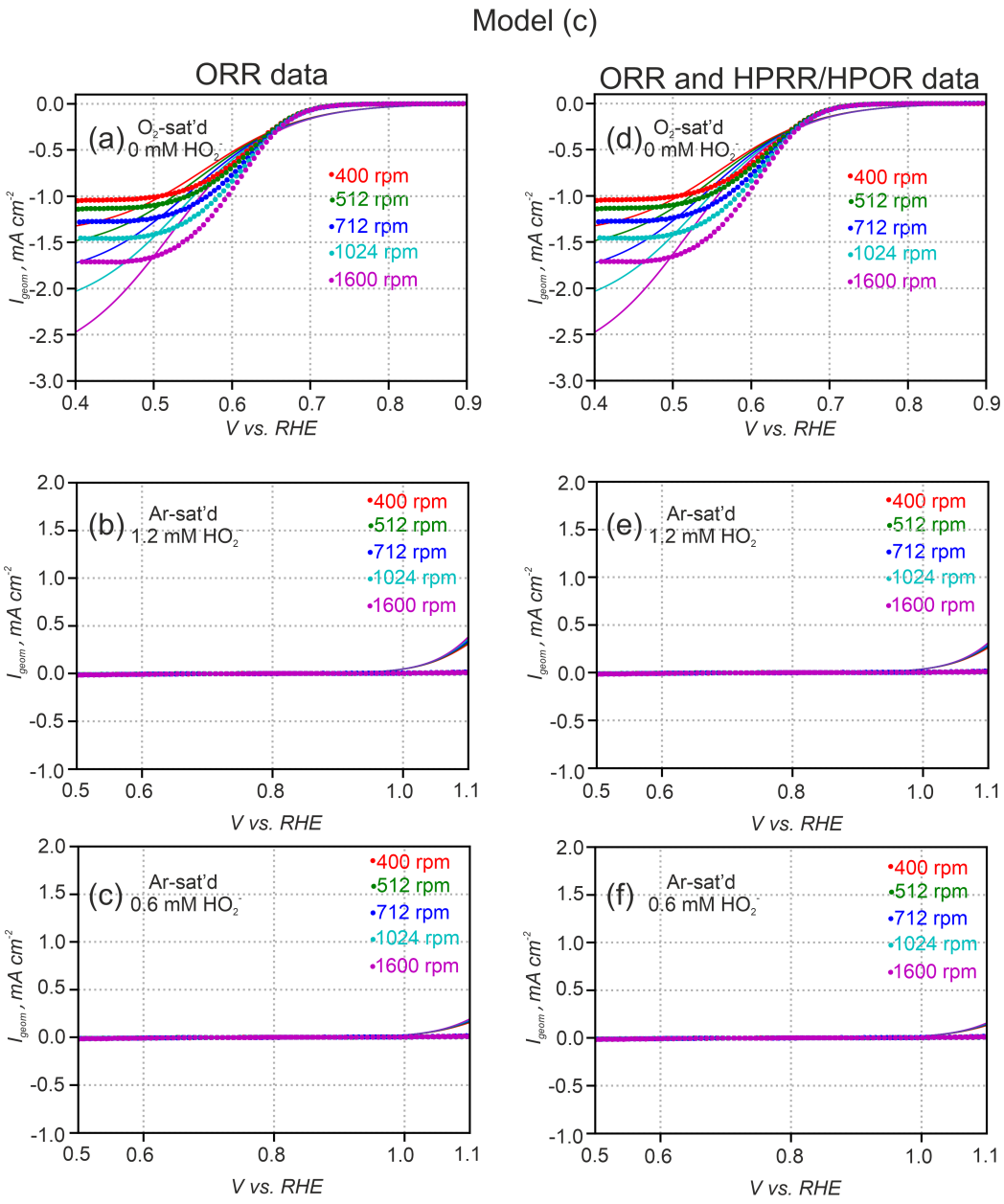

Supplementary Figure 6. Example of modeling results for the model (c) with a single step. All figures include the simulated RDE CVs for 10 random sets of model parameters with target functional lower than the experimental error (semi-transparent lines) and averaged experimental data (dots). Model parameters were adjusted by fitting of ORR RDE (a-c) and both ORR and HPRR/HPOR RDE (d-f) data. Simulated RDE CVs for O_2-saturated solution (a, d), Ar-saturated solution with added 1.2 mM (b, e) and 0.6 mM (c, f) of hydroperoxide are shown.

References.

1 V. G. Levich, *Physicochemical hydrodynamics*, Prentice Hall, Scripta Technica, Inc., Englewood Cliffs, N. J., 1962.

2 N. M. Marković, H. A. Gasteiger and P. N. Ross, *J. Phys. Chem.*, 1996, **100**, 6715–6721.

3 R.E. Davis, G.L. Horvath and C.W. Tobias, *Electrochim. Acta*, 1967, **12**, 287–297.

4 J. T. Mefford, A. A. Kurilovich, J. Saunders, W. G. Hardin, A. M. Abakumov, R. P. Forslund, A. Bonnefont, S. Dai, K. P. Johnston and K. J. Stevenson, *Phys. Chem. Chem. Phys.*, 2019, **21**, 3327–3338.

5 M. T. M. Koper and J. H. Sluyters, *J. Electroanal. Chem. Interfacial Electrochem.*, 1991, **303**, 73–94.

6 C. T. Alexander, A. M. Abakumov, R. P. Forslund, K. P. Johnston and K. J. Stevenson, *ACS Appl. Energy Mater.*, 2018, **1**, 1549–1558.